Beacons at the Gamma Ray Horizon

K. Mannheim[1], S. Westerhoff[2], H. Meyer[2], and H.-H. Fink[3]

[1] Universitäts-Sternwarte, Geismarlandstr. 11, D-37083 Göttingen, Germany
[2] Universität Wuppertal, Fachbereich Physik, D-42097 Wuppertal, Germany
[3] Max-Planck-Institut für extraterrestrische Physik, D-85740 Garching, Germany

Abstract. Blazars with redshifts $z \leq 0.1$ are likely candidates for detection at energies in the range 300 GeV – 50 TeV with Čerenkov telescopes and scintillator arrays. We present γ-ray flux predictions for a sample of 15 nearby flat-spectrum radio sources fitting the proton blazar model of Mannheim (1993a) to their observed broad-band spectral energy distributions. At high energies, we use fluxes or flux limits measured by ROSAT, CGRO and the Whipple Observatory to constrain their spectra. We take into account absorption of the γ-rays by pair production with low energy photons of the diffuse infrared-to-optical photon background produced by galaxies (cosmic absorption) and with low energy synchrotron photons of the blazar radiation field (internal absorption). Typically, the theoretical spectra decrease much faster above TeV (photon index $s \approx 3$) than between GeV and TeV ($s \approx 2$) owing to internal absorption.

The predicted fluxes are confronted with flux limits in the 20-50 TeV energy range obtained by the *High Energy Gamma Ray Astronomy* (HEGRA) experiment. Without cosmic absorption, the fluxes are about equal to the current sensitivity of HEGRA. Improved γ/hadron separation techniques could render a detection by HEGRA possible, if cosmic absorption by the far-infrared background at wavelengths $\sim 100~\mu$m is not exceedingly strong.

Key words: radiation mechanisms: non-thermal – instrumentation: detectors – BL Lacertae objects: general – cosmology: diffuse radiation – gamma rays: theory

1. Introduction

One of the most remarkable results obtained with the spark chamber experiment EGRET onboard the Compton Gamma Ray Observatory is the discovery of a large number of γ-ray point sources at high galactic latitudes (Fichtel et al. 1994, Montigny et al. 1995). Most of the sources have been identified as blazars, which comprise an important subclass of active galactic nuclei (AGN). Blazars are characterized by highly variable, featureless and polarized continuum emission. In the radio-to-soft X-ray range, the emission is commonly attributed to synchrotron emission from a collimated plasma jet (Blandford & Königl 1979) presumably emerging from the rotating magnetosphere of an accreting supermassive black hole of mass $M \sim 10^8$-$10^{10} M_\odot$ (Camenzind 1990). Due to relativistic bulk motion, the radiation pattern of the jet is sharply peaked about its axis. In blazars, the jet axis is aligned closely with the line-of-sight, leading to Doppler-boosted emission and superluminal motion of radio knots.

Recent multifrequency observations of blazars (Maraschi et al. 1994, Falomo et al., 1995, Valtaoja & Teräsranta 1995) show that mm, optical, X-ray and γ-ray lightcurves all trace the same event during a 'flare'. This favors a synchrotron-self-Compton (SSC) or proton-initiated-cascade (PIC, Mannheim et al. 1991) origin of the γ-rays at evolving shock fronts. Both mechanisms predict correlated TeV emission (Zdziarski & Krolik 1994, Mannheim 1996).

At high photon energies, the γ-radiation from remote cosmic sources is severely attenuated by pair production via $\gamma + \gamma \rightarrow e^+ + e^-$ on low energy background photons (Gould & Shrèder 1966). Stecker et al. (1992) propose to infer the diffuse near-infrared background radiation, which is difficult to observe directly, by measuring the expected TeV cutoff in the spectra of blazars at $z \approx 0.1$ owing to cosmic absorption. Salamon et al. (1994) argue that γ-ray measurements could also be used as a yardstick to determine the cosmic distance scale. MacMinn & Primack (1996) point out that the diffuse infrared-to-ultraviolet background is directly related to models of galaxy formation. Measuring the diffuse background from the infrared to the ultraviolet bands, requires observations of blazars at γ-ray energies from 10 GeV (Madau & Phinney 1996)
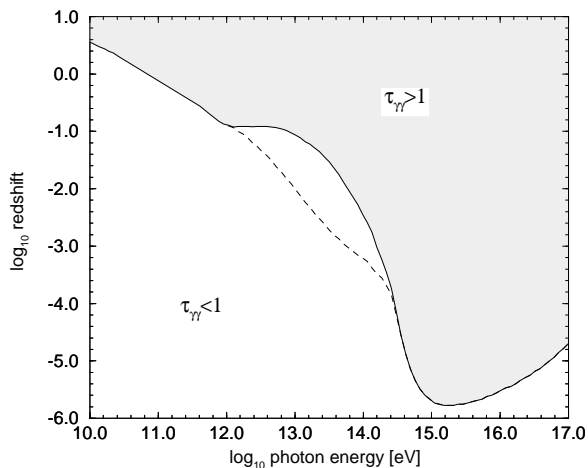
arXiv:astro-ph/9605107v1 17 May 1996

Fig. 1. The γ-ray horizons $\tau_{\gamma\gamma}(E, z) = 1$ corresponding to the two different diffuse background models shown in Fig.2. The horizons were calculated assuming $\Omega = 1$, $q_\circ = 0.5$, $H_\circ = 75$ km s^{-1} Mpc^{-1} and a photon number density evolving with redshift as $n'd\epsilon' = (1 + z)^3 nd\epsilon$ (conserved number of photons)

to 50 TeV. Probing the Universe with γ-rays will allow for independent tests of cosmological scenarios based on the well-understood physics of pair production.

Figure 1 shows the γ-ray horizon marking the relation between photon energy E and redshift z of a γ-ray source defined by $\tau_{\gamma\gamma}(E, z) = 1$. The solid curve is obtained by numerically integrating the optical depth $\tau_{\gamma\gamma}$ as given in Dwek & Slavin (1994) using the present-day background spectrum computed by averaging various galactic evolutionary scenarios of MacMinn & Primack (1996) shown in Fig.2. This spectrum remains well below current experimental limits for the near-infrared background (Biller et al. 1995). Practically, knowledge of the turnover energy E for a given redshift would yield the value of the diffuse background photon density above the resonant energy $\epsilon = 2m_e c^2/[E(1 + z)^2]$. Compared to our standard scenario for $E(z)$ shown as the solid line in Fig. 1, the turnover energy increases if (i) the Hubble constant has a value greater than 75 km s^{-1} Mpc^{-1}, (ii) the diffuse background radiation has a density lower than the value obtained by averaging the MacMinn & Primack models or (iii) the evolution of the diffuse background density $n'(\epsilon')d\epsilon' \propto (1 + z)^k$ is more shallow than $k = 3$ already for moderate redshifts (keeping $\Omega = 1$ and $\Lambda = 0$ fixed). A low background photon density would indicate late galaxy formation, and thus only a small amount of cold dark matter in the models of MacMinn & Primack. Effects (i)–(iii) can reduce the optical depth $\tau_{\gamma\gamma}(E, z)$ by a maximum factor of ~ 3 below the values adopted in the present work assuming the extremal values $H_\circ = 100$ km s^{-1} Mpc^{-1}, a present-day infrared background equal to the integrated

number counts of IRAS galaxies (de Zotti et al. 1995) and $k = 0$.

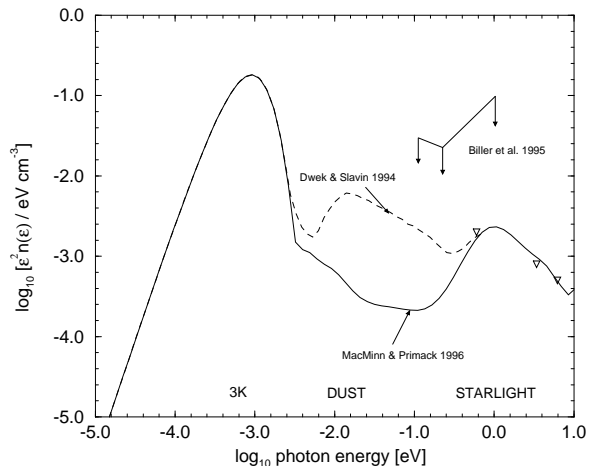By inspection of Fig. 1 it is obvious that sources at red-

Fig. 2. *Solid line:* the infrared-to-ultraviolet diffuse background radiation field adopted in the present work. *Dashed line:* a diffuse background assuming that the γ-ray spectrum of Mrk421 cuts off at TeV due to cosmic absorption. Triangles denote estimates by Madau & Phinney (1996) of the optial-to-ultraviolet diffuse background based on deep galaxy surveys

shifts less than ~ 0.1 are required to pin down the γ-ray horizon in the TeV range. Several low-redshift EGRET blazars have been found, of which Mrk421 and Mrk501 have also been detected at TeV energies (Punch et al. 1992, Quinn et al. 1996), and many more potential sources with similar overall spectrum exist. To extract information on the intergalactic absorption from observed TeV spectra requires detailed knowledge of the spectra intrinsic to the sources.

In this paper, we therefore investigate a sample of nearby flat-spectrum radio sources by fitting the proton blazar model of Mannheim (1993a) to their multifrequency spectra. In Sect.2 we briefly outline the model and explain the fitting procedure. In Sect.3, we introduce the sample and proceed in Sect.4 comparing the predicted fluxes above TeV with the sensitivity of HEGRA. Finally, we summarize our results on the feasibility of mapping the γ-ray horizon in the TeV range.

2. Outline of the proton-initiated cascade model

Recent multifrequency observations of blazars seem to support an explanation of their γ-ray emission in terms of relativistic shocks propagating down an expanding jet (at least this is a powerful and predictive working hypothesis). Multiple shocks (Courant & Friedrichs 1948) can

form behind a magnetic nozzle (van Putten 1995). Particle acceleration at relativistic and oblique shocks by diffusive and drift mechanisms has been studied by Kirk & Heavens (1989), Schneider & Kirk (1989), Kirk & Schneider (1989), Webb (1989), Begelman & Kirk (1990), Krülls (1990), Kirk (1992), Ellison et al. (1995). In the innermost regions of the jet, at the beginning of an outburst, the shocks seem to emit an optically thin mm-to-optical synchrotron spectrum (in some cases reaching up to soft X-rays) with an associated X-to-γ-ray spectral component which can dominate the emitted power. Further down the jet, the shocks become transparent to radio synchrotron emission so that the initial outburst shows up delayed and broadened in radio lightcurves. Morphologically, the radio outbursts seem to be associated with the birth of new knots in VLBI maps.

It is tantalizing to identify the high energy spectral component with the inevitable synchrotron-self-Compton emission from the traveling shocks. However, this would require that the photon energy density exceeds the magnetic energy density in sources where the γ-ray luminosity exceeds the optical luminosity, i.e. $u_{\rm rad} \gg u_{\rm B}$, since

$$L_{\rm ssc} \simeq \frac{u_{\rm rad}}{u_{\rm B}} L_{\rm syn} \tag{1}$$

The same conclusion $u_{\rm rad} \gg u_{\rm B}$ follows from assuming that TeV photons are singly scattered optical synchrotron photons. Since $x_{\rm opt} = h\nu/(m_{\rm e}c^2) = 3.4\,10^{-14}B_\perp\gamma^2$ and $x_{\rm tev} = \frac{4}{3}x_{\rm opt}\gamma^2$, we obtain $B_\perp = 3\,10^{13}x_{\rm opt}^2/x_{\rm tev}$ G $\approx 3\,10^{-3}$ G corresponding to the comoving-frame magnetic energy density of $\sim 4\,10^{-7}\gamma_{\rm j}^{-2}$erg cm^{-3}. This value is negligible compared to the comoving-frame radiation energy density ~ 1 erg s^{-1} (Sect.3.2). However, the energy density of the relativistic electrons $u_{\rm rel}$ should certainly exceed the energy density $u_{\rm rad}$ of the photons they produce implying $u_{\rm rel} \gg u_{\rm B}$. This raises the problem of how $u_{\rm rel}$ can be maintained at such a high level in a quasi-stationary situation. The commonly invoked mechanism of diffusive acceleration does not operate at $u_{\rm rel} \gg u_{\rm B}$, since particles diffuse by pitch-angle scattering off magnetic field fluctuations. The pressure of these fluctuations is expected to be near the saturation value $u_{\delta B} \approx u_{\rm B}$, thus imposing the condition $u_{\rm rel} \leq u_{\rm B}$.

This conceptual problem with the SSC mechanism is removed if it is assumed that protons instead of electrons scatter off the synchrotron photons. In interstellar space, the energy in relativistic protons largely exceeds the energy in electrons which could also be true in radio jets. The reasons for this are unclear. However, if the proton acceleration mechanism can tap the Maxwell tail of a thermal distribution (Malkov & Völk 1995), it is plausible that the proton energy density will generally be larger than the electron energy density. Protons in a high radiation density environment, such as the shocks presumably traveling down radio jets, produce ample pions and pairs by inelastic scattering off the electronic synchrotron photons

if they reach high energies $\sim 10^{8-11}$ GeV (Biermann & Strittmatter 1987).

The pairs and pions initiate electromagnetic cascades (Mannheim et al. 1991) at the shocks. For a simple Blandford & Königl (1979) type jet, the predicted spectra match the observed spectra from radio frequencies to γ-rays very well (Mannheim 1993a). Contrasting any other model predicting γ-rays from blazars, the proton blazar model implies source spectra reaching > TeV photon energies *generally*. Internal absorption of the γ-rays above TeV by the low energy electronic synchrotron photons leads to a steepening of the spectra by one power above TeV ($s \approx 3$). The PIC flux varies simultaneously with the flux of the infrared-to-optical target photons and with the proton maximum energy.

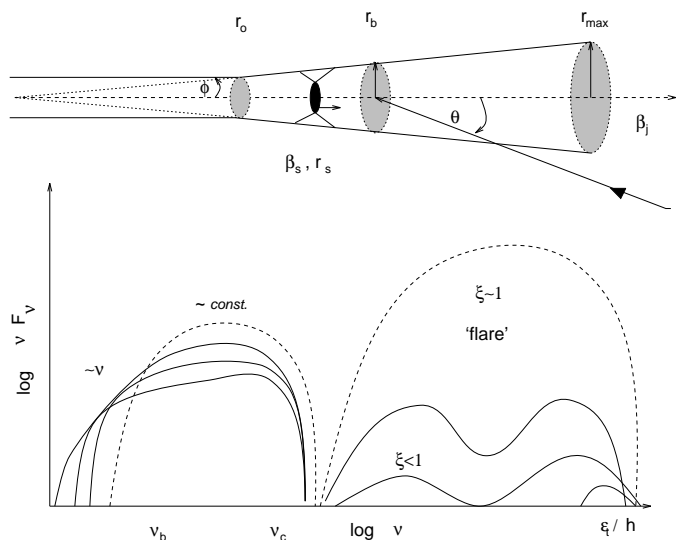Denoting the emission volume as V (assumed to be equal

Fig. 3. Sketch of jet geometry and typical synchrotron + PIC spectrum. *Solid lines* show the emission from various r in the range $r_{\rm b} \leq r \leq r_{\rm max}$. *Local* electronic synchrotron spectra are characterized with increasing frequency by a synchrotron-self-absorption turnover, an optical thin $S_\nu \propto \nu^{-1/2}$ radio/mm spectrum, a $S_\nu \propto \nu^{-1}$ infrared spectrum and a steep near-infrared/optical/UV spectrum. The superposition of many such spectra along the expanding jet yields a flat radio spectrum with $S_\nu \propto const.$ and a $S_\nu \propto \nu^{-1}$ spectrum above the break frequency $\nu_{\rm b}$ turning over steeply at $\nu_{\rm c}$. The corresponding PIC spectrum rises roughly as $S_\nu \propto \nu^{-(0.5-0.9)}$ (depending on the pair creation optical depth $\tau_{\gamma\gamma}$) and steepens in the MeV to GeV range where $S_\nu \propto \nu^{-1}$ is typical. Above $\sim$ TeV, the PIC spectra steepen further by one power and then cut-off at ultra high energies. *Dashed lines* indicate the spectrum emitted when a newly formed shock ($\xi \sim 1$) enters the region at $r = r_{\rm b}$ where the target density for proton cooling rises sharply (the synchrotron radiation at target frequencies becomes optically thin at this point). Further down the jet, the γ-ray luminosity decreases, since the proton maximum energy required for $\xi \sim 1$ cannot be maintained by the nonlinearly evolving shocks

for protons and electrons), the energy density ratio of protons and electrons as $\eta = u_{\mathrm{p}}/u_{\mathrm{e}}$ ($\eta \approx 100$ in the Milky Way at GeV energies) and the ratio of electron and proton cooling times as $\xi = t_{\mathrm{e}}/t_{\mathrm{p}}$, the PIC luminosity can be expressed in terms of the SSC luminosity Eq.(1) by

$$L_{\mathrm{pic}} \simeq u_{\mathrm{p}}Vt_{\mathrm{p}}^{-1} = \eta u_{\mathrm{e}}Vt_{\mathrm{p}}^{-1} \simeq \eta L_{\mathrm{syn}}t_{\mathrm{e}}t_{\mathrm{p}}^{-1} = \eta\xi L_{\mathrm{syn}} \qquad (2)$$

The cooling time ratio ξ depends strongly on the maximum particle energies, since $t_{\mathrm{cool}} \propto 1/\gamma$ where γ denotes the Lorentz factor of the particle. Balancing cooling and expansion time scales for protons and electrons (so that $\xi = 1$) yields extremely large proton Lorentz factors $\gamma_{\mathrm{p}} \sim 10^{8-11}$. In the case of $\xi = 1$, the PIC luminosity can exceed the SSC luminosity by the, possibly large, proton-to-electron ratio η. A crucial requirement is, of course, that acceleration is faster than expansion and that the Larmor radius of the gyrating particles does not exceed the radius of curvature of the shocks (Bell 1978). The latter criterion hurts protons more than electrons, since the proton Larmor radius is much larger than the electron Larmor radius. If the coherent shock structure is destroyed during the nonlinear evolution of the shock propagating down the jet, proton scattering at the maximum energy becomes inefficient (scattering length $\sim$ Larmor radius in Bohm diffusion). We therefore expect that $\xi(t) \propto \gamma_{\mathrm{p,max}}/\gamma_{\mathrm{e,max}}$ is decreasing with time. Multiple shocks generate some time-average $\langle\xi\rangle$ which will be relevant for our sample of randomly observed blazars.

We compute the cascade spectra numerically as described in Mannheim et al. (1991) and Mannheim (1993a), but taking into account additionally Bethe-Heitler pair production and proton synchrotron radiation assuming a photo-pair luminosity $L_{\mathrm{e\pm}} \simeq 0.5L_{\pi}$ (strictly valid only for straight $\alpha = 1$ power law photon fields as a target; Sikora et al. 1987). The optical depth of the jet with respect to pair creation is computed as follows: Since the typical angle of emission in the comoving frame is $\theta' \approx \pi/2$, the intersection of the line of sight with the jet corresponds to its transverse radius r (denoted as $r_{\perp}$ in Mannheim 1993a). The target radiation (>far-infrared) becomes optically thin at $r = r_{\mathrm{b}}$ where we expect the largest γ-ray luminosity to be produced (see caption of Fig.3). The comoving-frame optical depth is then given by

$$\tau'_{\gamma\gamma} = n'_{\mathrm{syn}}\sigma_{\gamma\gamma}r_{\mathrm{b}} = au_B\epsilon'^{-1}_{\circ}\ln[\nu_{\mathrm{c}}/\nu_{\mathrm{b}}]^{-1}\sigma_{\gamma\gamma}r_{\mathrm{b}} \qquad (3)$$

where

$$a = \frac{u_{\mathrm{syn}}}{u_{\mathrm{B}}} \simeq \gamma_{\mathrm{j}}\beta_{\mathrm{j}}\phi\left(1 + \eta\Lambda_{\mathrm{e}}/\Lambda_{\mathrm{p}}\right)^{-1} \qquad (4)$$

(cf. Eq.(24) in Blandford & Königl 1979). The pair-creation cross section reaches $\sigma_{\gamma\gamma} \simeq \frac{1}{3}\sigma_{\mathrm{T}}$ at the resonant target photon energy $\epsilon'_{\circ} = 2(m_{\mathrm{e}}c^2)^2/E'$ for a γ-ray with energy E'. Using the Lorentz invariance of the optical depth, i.e. $\tau_{\gamma\gamma}(E) = \tau'_{\gamma\gamma}(E')$, we obtain the optical depth in the observer's frame. Synthetic cascade spectra were

produced with the following input parameters: redshift z, jet Lorentz factor γ_{j}, angle to the line of sight θ, proton-to-electron cooling rate ratio ξ, proton-to-electron energy density ratio η, jet luminosity L_{jet} (magnetic field + relativistic particles), synchrotron cutoff frequency in the comoving frame ν'_{c}. While ξ affects only the cascade part of the spectrum, η also affects the electronic synchrotron spectrum for fixed L_{jet}, since it imparts the given energy between electrons and protons. In general, the synchrotron and cascade spectrum are both rather robust. The most important effect is the dramatic variation of the observed flux for variations with the boosting angle θ. Variations of the cosmological parameters Ω, Λ and $H_{\circ}$ from their adopted values 1, 0 and 75 km s^{-1} Mpc^{-1} do not significantly affect the model fits, they do affect the luminosities in Tab.2 accordingly.

3. Multifrequency modeling of nearby blazars

3.1. The sample

We investigated the spectra of blazars from the list of Fichtel et al. (1994) which have a redshift $z \leq 0.1$ or unkown, and which are visible from the northern hemisphere. The sources typically have a flat or inverted radio spectrum > 1 Jy. We used published multifrequency data, ROSAT data from the all-sky survey as well as from public pointings, preliminary flux limits from Whipple observations and HEGRA scintillator and AIROBICC flux limits. At the time of writing, 5 out of a total of 15 sources were detected by EGRET, $2 = $ Mrk421 and Mrk501 were detected by Whipple (Punch et al. 1992, Kerrick et al. 1995b, Quinn et al. 1996). Recently, the detection of Mrk421 has been confirmed independently by the HEGRA Čerenkov telescopes (Petry et al. 1995). Extending the sample to $z = 0.2$ would roughly double the number of sources.

To estimate the effect of intergalactic absorption, we assumed $z = 0.3$ for those sources, where no redshift was available. At $z < 0.3$, the corresponding host galaxies are generally expected to be seen. We used the mean diffuse background density shown in Fig.2 for the computation of the absorption.

The data sets are neither simultaneous nor complete, and the intrinsic source variability, which shows up as a large dispersion of the fluxes for a given photon energy (e.g. TeV outburst of Mrk421 by a factor of ~ 10; Kerrick et al. 1995b, Macomb et al. 1995), brackets the theoretical spectrum. Since dust-rich quasars such as 3C273 (Lichti et al. 1995, Mannheim 1993b) are not present in our sample, additional absorption of the γ-rays by infrared photons from the host galaxy can be neglected. Predictions of TeV fluxes are given within the above uncertainties which may well add up to a factor of $\sim$a few. Table 1 summarizes the high energy measurements of the sources comprising our sample.
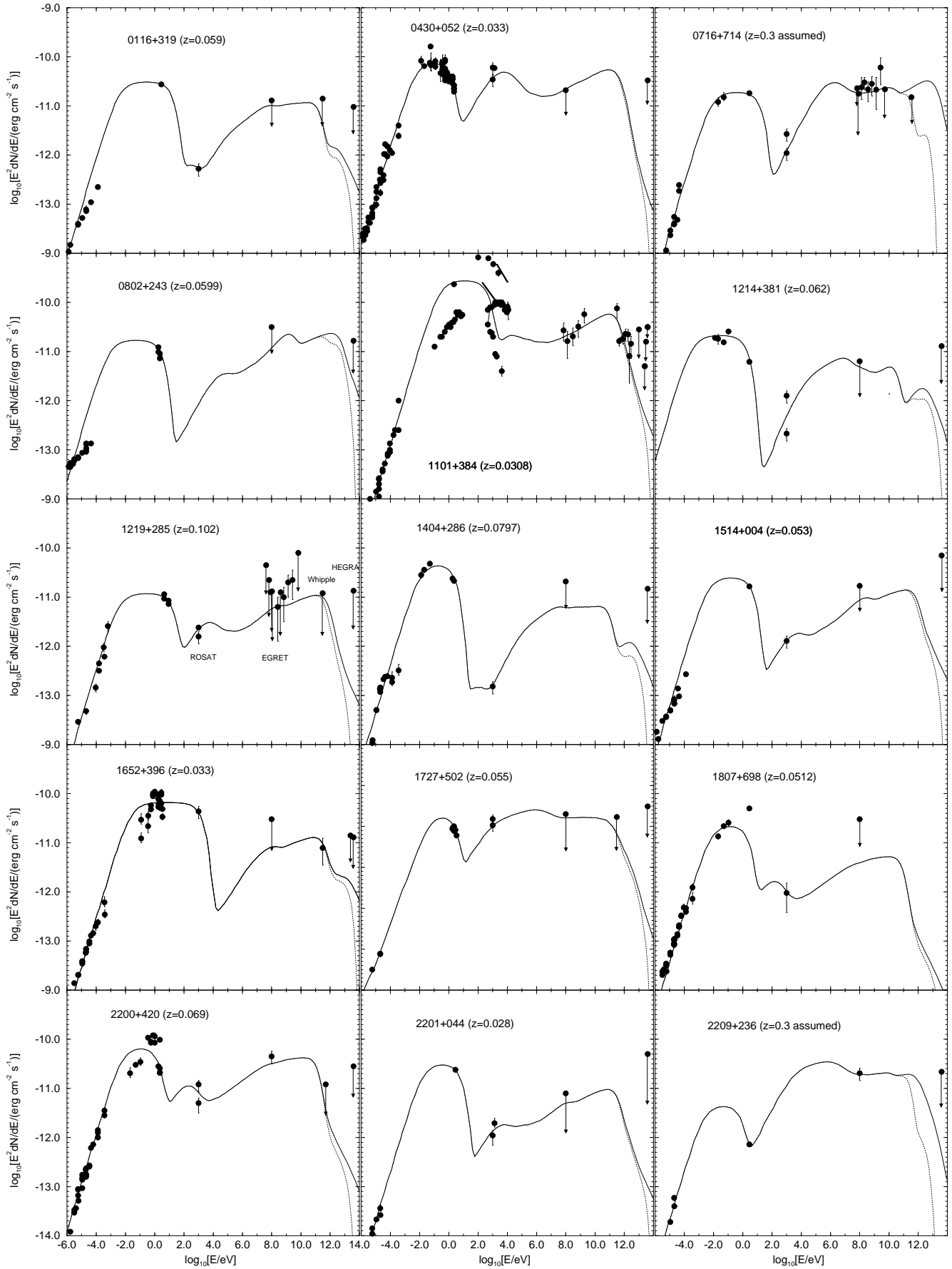
Fig. 4. *Solid lines:* proton blazar model fits. *Dotted lines:* same model fits with external (cosmic) absorption taken into account

Table 1. Summary of high-energy data available for northern blazars with $z \leq 0.1$ or unkown redshifts. The numbers in the columns below the experiments give the observed differential energy flux or flux limit $\log_{10}[\mathrm{E}^2 \mathrm{dN/dE}\ (\mathrm{erg\ cm}^{-2}\ \mathrm{s}^{-1})]$ at the threshold energy of the respective experiment

Source	Redshift	ROSAT[a]	CGRO[b]	Whipple[c]	HEGRA[d]	Tibet[e]
0116+319 (MS 01166+31)	0.059	−12.3	< −10.9	< −10.9	< −11.0	–
0430+052 (3C120.0)	0.033	−10.2	< −10.7	–	< −10.5	–
0716+714	–	−11.6	−10.5	< −10.8	–	–
0802+243 (3C192.0)	0.0599	–	< −10.5	–	< −10.8	–
1101+384 (Mrk421)	0.0308	−10.0	−10.6	−10.8	< −10.5	< −10.6
				AIROBICC:	< −11.3	
1214+381 (MS 12143+38)	0.062	−12.7	−11.2	–	< −10.9	–
1219+285 (ON 231)	0.102	−11.8	−10.6	< −10.9	< −10.9	–
1404+286 (OQ 208)	0.0797	−12.8	< −10.7	–	< −10.8	–
1514+004 (PKS 1514+00)	0.053	−11.9	< −10.8	–	< −10.2	–
1652+398 (Mrk501)	0.033	−10.3	< −10.5	−11.1	< −10.9	–
				AIROBICC:	< −10.8	
1727+502 (II Zw 077)	0.055	−10.8	< −10.7	< −10.8	< −10.5	–
1807+698 (3C371.0)	0.0512	−12.0	< −10.5	–	–	–
2200+420 (BLLac)	0.069	−10.9	−10.3	< −10.9	< −10.6	–
2201+044 (PKS2201+04)	0.028	−11.9	< −11.1	–	< −10.3	–
2209+236	–	–	−10.7	–	< −10.7	–

[a]   PSPC differential flux at 1 keV adopting $\alpha = 0.5$ ($S_\nu \propto \nu^{-\alpha}$)

[b]   EGRET differential flux at 100 MeV adopting $\alpha = 1$; Fichtel et al. (1994), Thompson et al. 1995, Montigny et al. (1995)
    For BL Lac, we give a preliminary EGRET flux (Hartman 1995)

[c]   Čerenkov telescope data at a threshold energy of 0.35 TeV adopting $\alpha = 2$; Kerrick et al. (1995a)

[d]   Scintillator array data at the threshold 40 TeV adopting an exponentially decreasing spectrum
    For Mrk 421 and Mrk 501 we also give the AIROBICC data for $E_{\mathrm{th}} \simeq 25$ TeV
    Data are from Kühn (1994), Karle et al. (1995) and Westerhoff et al. (1995b) on behalf of the HEGRA collaboration

[e]   Differential flux from air shower data at 10 TeV adopting an exponential spectrum; Amenomori et al. (1994)

3.2. Summary of results

The data used to obtain the model fits are non-simultaneous and there are large gaps in frequency coverage. Therefore, the parameter choices, and hence the spectra, are not free of ambiguities. The accuracy of the model predictions cannot be much better than to a factor of ∼a few. Nevertheless, some important results can be inferred from the model fits:

Gamma-to-optical luminosity ratios: Among the randomly sampled nearby blazars, there is no source with a strong γ-flare. The γ-ray luminosities are $L_\gamma \approx \eta\xi L_{\mathrm{opt}} \approx L_{\mathrm{opt}}$ with a proton-to-electron ratio $\langle\eta\rangle = 80 \pm 30$ and $\langle\log_{10}[\xi]\rangle = -1.8 \pm 0.5$. The absence of flares could be due to either a low duty cycle for $\xi \approx 1$ states or, alternatively, the acceleration process could generally be less efficient in BL Lacertae objects than in radio quasars (most nearby blazars in our sample are BL Lacertae objects). This could be related to the magnetic field structure which is preferentially perpendicular to the jet axis in low-luminosity BL Lacs and parallel in high-luminosity quasars (Bridle & Perley 1984).

TeV γ-rays: We note that promising candidates for detection at TeV energies are 0802+243, 0430+052, 1514+004 and 1219+285 (in addition to Mrk421 and Mrk501). The TeV photon flux predicted for 0716+714 accounting for cosmic absorption at $z = 0.3$ is similar to that for 1219+285. However, we consider this redshift as a lower limit implying that the cosmic absorption is likely to be much stronger than assumed.

Spectral slope between TeV and 50 TeV: Above TeV, the spectra continue as power laws, but with a steeper slope. The intrinsic source spectrum is given by $I_{\mathrm{s}} = I_\circ(1 - \exp[-\tau_{\gamma\gamma,\mathrm{int}}])/\tau_{\gamma\gamma,\mathrm{int}}$ corresponding to absorption in a homogeneous source, for which the photospheric size is energy-dependent. Hence, for $\tau_{\gamma\gamma,\mathrm{int}} \gg 1$ and since $\tau_{\gamma\gamma,\mathrm{int}} \propto E$, the asymptotic spectrum is given by $I_{\mathrm{s}} \propto I_\circ/E$. This is in marked contrast to the external absorption, which is given by an exponential law, i.e. $I_{\mathrm{obs}} = I_{\mathrm{s}}\exp[-\tau_{\gamma\gamma,\mathrm{ext}}]$.

Similarity of comoving-frame spectra: Somewhat surprising, we find that the comoving-frame break frequencies are roughly constant with $\nu'_{\mathrm{b}} \approx 10^{11}$ Hz. The comoving-frame cutoff frequencies also agree with a constant value of $\nu'_{\mathrm{c}} \approx 3\,10^{14}$ Hz, which is theoretically expected from non-relativistic theory (Biermann & Strittmatter 1987). This could be a hint that the physics in the comoving frame of the relativistic inner jet is basically the same as in the (non-relativistic) hot spots of the jet hundreds of kiloparsecs away from the origin of the jet (Harris et al. 1994).

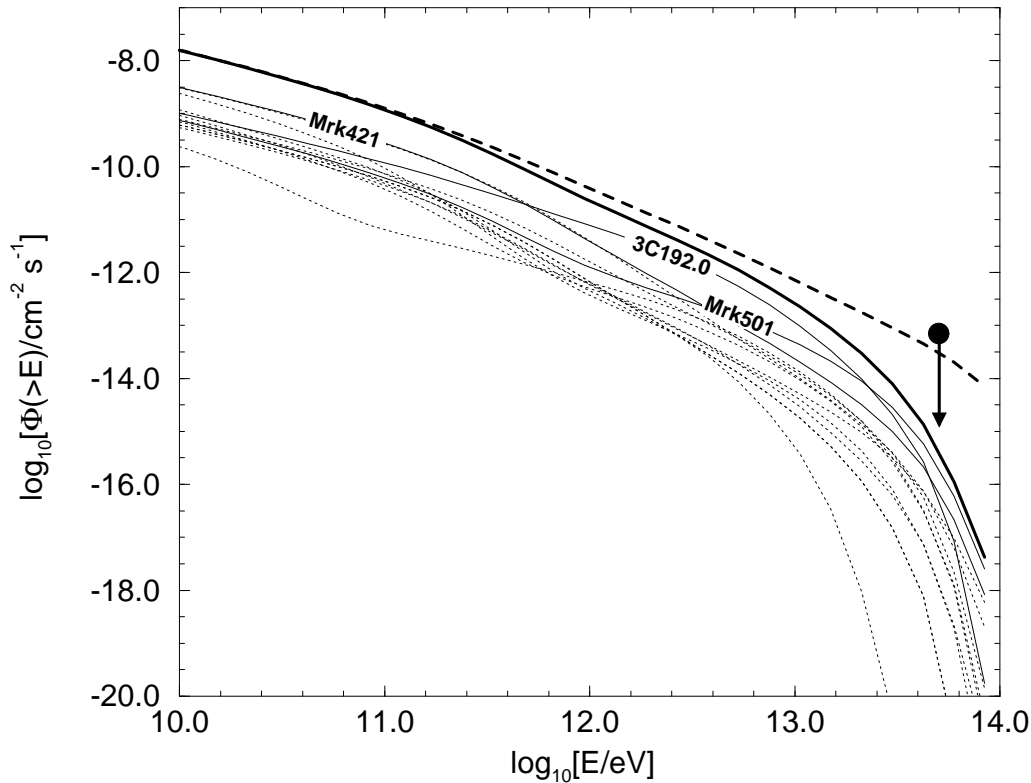*Proton maximum energy:* The average proton maximum

Fig. 5. Integral fluxes and cumulative HEGRA flux limit of the 13 blazars visible at La Palma (excluding 0716+714 and 1807+698) from 10 GeV to 100 TeV. *Dashed bold line:* sum of fluxes with internal absorption. *Solid bold line:* sum of fluxes with internal+external absorption

energy in the observer's frame inferred from the fits is $\sim 10^{10}$ GeV. Detection of the resulting neutrino background from blazars seems possible (Mannheim 1995).

Jet Lorentz factor: The average jet Lorentz factor $\langle\gamma_j\rangle_{obs} = 10 \pm 4$ is consistent with the value $\gamma_j = 7$ inferred for low-luminosity radio sources based on the unification of BL Lacs with Fanaroff-Riley type I galaxies (Urry & Padovani 1995). A freely expanding jet should have $\Phi \approx \gamma_j^{-1} \approx 6$ deg which is consistent with the value from the fits.

Variability time scales: From the model fits and Eq.(4) we obtain the typical numbers $\langle u_{syn}/u_B\rangle = 0.01$, $\langle B\rangle = 40$ G, $\langle r_b\rangle = 10^{15}$ cm and the Doppler factor $\langle\delta\rangle = 10$. Using Eq.(3), we obtain the γ-ray break energy $\langle E\rangle = \langle\delta\rangle\langle E'\rangle = 1$ TeV where intrinsic absorption sets in $(\tau'_{\gamma\gamma}(E') = 1)$. These numbers imply a minimum variability time scale $\langle\Delta t_{obs}\rangle = \langle r_b\rangle(1 + z)/(\langle\delta\rangle c) \approx 3\,10^3$ s in the observer's frame.

4. Current flux limits

In the TeV energy region, the search for point sources is only possible using earth-bound experimental setups sensitive to the secondary particles induced by cosmic ray primaries in the Earth's atmosphere. The main task is to separate the air showers induced by primary γ's from the much more abundant hadronic showers. Apart from detecting the charged secondary particle component using a matrix of scintillator counters, the photons of the Čerenkov light cone produced by relativistic electrons also give valuable complementary information about the shower and thus the incoming primary particle. Whereas up to now, scintillator arrays have provided only upper limits for the flux from γ-ray point sources, the employment of imaging Čerenkov telescopes has been the most successful ground based observation technique of the last years: observation of ultra high energy γ-radiation from the Crab nebula, Mrk421 and Mrk501 are reported. As an example for experimental setups searching for TeV γ-rays, we quote the results obtained by the HEGRA detector array located on the Canary Island La Palma (28.8 N, 17.7

Table 2. Physical parameters for the model fits shown in Fig.4 and predicted high-energy γ-ray fluxes. The last four columns give the predicted integral γ-ray fluxes above 1 and 40 TeV in units of 10^{-14}cm^{-2} s^{-1} accounting for *internal* absorption (index i) and (ii) *internal + external* absorption (index a) adopting the same differential spectra as noted in Tab.1

Source	γ_j	$\frac{\theta}{\deg}$	$\frac{\phi}{\deg}$	$\log_{10}\left[\frac{L_{\text{jet}}}{\text{erg/s}}\right]$	η	$\log_{10}[\xi]$	$\log_{10}\left[\frac{\nu'_c}{\text{Hz}}\right]$	$F_i(>\text{TeV})$	$F_a(>\text{TeV})$	$F_i(>40\text{TeV})$	$F_a(>40\text{TeV})$
0116+319	6	6	7	44.8	110	-2.1	14.8	50	30	0.5	$3\,10^{-2}$
0430+052	8	8	5	45.0	30	-1.3	13.8	600	400	0.2	$5\,10^{-2}$
0716+714	16	2	1	44.5	70	-1.3	14.4	900	80	20	$6\,10^{-9}$
0802+243	4	3	2	44.0	80	-1.5	14.1	500	500	4	$2\,10^{-1}$
1101+384	20	2	5.7	45.2	50	-2.2	15.8	500	400	0.6	$1\,10^{-1}$
1214+381	5	15	5	45.7	100	-2.2	14.2	50	30	0.6	$2\,10^{-2}$
1219+285	10	7	4	45.2	100	-1.8	14.8	200	80	0.2	$7\,10^{-4}$
1404+286	10	3	4	44.7	100	-2.5	13.7	40	20	0.4	$7\,10^{-3}$
1514+004	7	5	3.5	44.5	100	-2.0	14.2	200	200	0.6	$4\,10^{-2}$
1652+398	10	2	3	43.9	100	-2.5	16.5	100	100	1.8	$6\,10^{-2}$
1727+502	10	5	10	44.0	30	-1.1	13.8	80	60	0.08	$6\,10^{-3}$
1807+698	10	9	5.7	44.9	30	-1.8	14.1	4	3	0.02	$1\,10^{-3}$
2200+420	10	7	10	45.6	100	-1.9	13.8	50	30	0.2	$6\,10^{-3}$
2201+044	10	5	4	44.0	90	-2.2	14.3	70	60	0.2	$4\,10^{-2}$
2209+236	10	7	5	45.7	100	-0.8	13.6	400	40	0.7	$1\,10^{-10}$
mean	10	6	5	44.8	80	-1.8	14.4				
variance	4	3	3	0.6	30	0.5	0.7				

W, 2200m a.s.l.). As it comprises a scintillator array of 224 counters, 17 Geiger towers for γ/hadron separation, and a 7×7 matrix of open Čerenkov counters (AIRO-BICC), HEGRA is able to equally exploit the information provided by the Čerenkov photons and the charged particle component of air showers. The observation of single objects is furthermore possible by the use of 3 Čerenkov telescopes which form the first part of a system of 5 telescopes. The operation of AIROBICC is restricted to clear, moonless nights, but the solid angle acceptance of about 1 sr allows to observe a large number of sources simultaneously. As AIROBICC and scintillator arrays are sensitive to different physical properties of air showers, they have different energy thresholds: the scintillator array detects showers with more than about 40 TeV energy of the primary particle, the threshold for AIROBICC is at about 20 TeV. As a consequence of the lower Čerenkov light yield and larger fluctuations in proton showers, the threshold energy for proton induced showers exceeds the γ-shower thresholds by about 10 TeV. The upper flux limits for γ-point sources from the AIROBICC array are of the order 10^{-13}cm^{-2}s^{-1} with γ-shower energy thresholds of about 25 TeV. For the extragalactic sources Mrk421 and Mrk501 AIROBICC provides upper flux limits of $1.24\,10^{-13}$ cm^{-2} s^{-1} and $3.72\,10^{-13}$ cm^{-2} s^{-1} at threshold energies of 25.3 and 24.0 TeV respectively (Karle et al. 1995). For the scintillator array, Kühn (1994) gives an upper flux limit of $4.3\,10^{-13}$ cm^{-2} s^{-1} above 40 TeV for Mrk421. The results quoted above were obtained without any attempt to reduce the large background of hadron induced showers, which are about 10^5 times more numerous than γ-induced showers.

Current data analysis applying cuts on the basis of γ/hadron- separation techniques (Westerhoff et al. 1995a) yields a cumulative flux limit of $7\,10^{-14}$ cm^{-2} s^{-1} (90% CL) above 50 TeV for the sum of the sources in our sample excluding 0716+714 and 1807+689 with poor visibility at La Palma (Westerhoff 1995b). This is approximately equal to the sum of the *unabsorbed* theoretical fluxes derived from the model fits (Fig.5, Tab.2). Accounting for absorption, the theoretical flux drops by roughly an order of magnitude lower. It is difficult to assess the systematical errors in the determination of the experimental flux sensitivity, but they can be estimated to be quite large. Since the theoretical errors are also difficult to control better than within factors of $\sim$a few by the very nature of the variable blazars, a detection of blazars at $\sim$50 TeV does not seem beyond reach. On the other hand, very strong absorption, such as proposed by Stecker et al. (1992) and Dwek & Slavin (1994) indicated as the dashed lines in Figs. 1 and 2, would further reduce the predicted flux above 50 TeV by orders of magnitude. In this case, detection of blazars at HEGRA scintillator energies would be truly impossible.

Future analysis will include methods to increase the signal-to-background-ratio by fully exploiting the information of all components of the experimental setup and by employing new and improved methods of data analysis.

5. Conclusions

The continuum spectra of 15 nearby blazars have been modeled satisfactorily over $\sim$ 20 orders of magnitude in frequency combining proton-initiated unsaturated synchrotron cascades and electron synchrotron radiation emitted by relativistic jets with a mean Lorentz factor

$\langle\gamma_j\rangle = 10 \pm 4$. The γ-ray spectra are complex, but a mean power law photon index $s \approx 2$ represents the spectra in the EGRET range rather well. The inferred physical parameters are in line with a proton-to-electron energy density ratio $\langle\eta\rangle = 80 \pm 30$. The proton cooling rate is less than the electron cooling rate by a factor $\sim 0.016^{+0.034}_{-0.011}$ implying about equal infrared-to-optical and γ-ray luminosities from the same emission volume.

Internal absorption of the γ-rays by the low energy synchrotron photons leads to a steepening of the spectra at $\sim$ TeV above which $s \approx 3$ up to ~ 100 TeV. The TeV spectra of Mrk421 and Mrk501 are not significantly affected by cosmic absorption and should have $s \simeq 3.2$.

Cosmic absorption *must* be present in 0716+714 for which the predicted TeV emission without absorption greatly exceeds the Whipple limit. Cosmic absorption becomes sufficiently strong for 0716+714 if its redshift is greater than 0.3.

Without cosmic absorption, the sum of the blazar fluxes is about equal to the current sensitivity of the HEGRA array. Taking into account cosmic absorption based on models of galaxy formation by MacMinn & Primack (1996), the predicted flux falls an order of magnitude below the current flux limit. The absorption at ~ 50 TeV is not very sensitive to cosmological parameters (e.g., Ω or Λ). A Hubble constant of 100 km s^{-1} Mpc^{-1} and late-epoch galaxy formation producing an infrared background equal to that produced by IRAS galaxies would increase our theoretical γ-ray fluxes by a factor of ~ 3. A mild enhancement of the theoretical flux is expected from forward cascading of the pairs produced in the intergalactic medium by inverse-Compton scattering off background photons (Protheroe & Stanev 1993, Aharonian et al. 1994, Plaga 1995), if the intergalactic magnetic fields are weak.

A critical appraisal of the systematic errors in the determination of the exact HEGRA energy threshold and flux level as well as the variable nature of the blazars leads us to conclude that detection of the nearest blazars with the HEGRA array seems feasible. A positive detection would disprove any claims of an exceedingly strong cosmic infrared background (with profound implications on the era of galaxy formation) and would provide strong support for a baryon-induced cascade origin of the γ-rays from blazars.

Note added in proof: After submission of the manuscript, we became aware of a preprint by Puget et al. (1996, A&A, in press), claiming the detection of a diffuse FIR background using COBE data. Within the uncertainties, their measured flux is equal to the far-infrared flux of the mean MacMinn & Primack background spectrum used in our paper.

References

Aharonian, F. A.; Coppi, P. S., Völk, H. J., 1994, ApJ 423, L5
Amenomori, M., et al., 1994, ApJ 429, 634
Begelman, M. C., Kirk, J. G, 1990, ApJ 353, 66
Bell, A.R., 1978, MNRAS 182, 443
Biermann, P.L., Strittmatter, P.A., 1987, ApJ 322, 643
Biller, S.D., Akerlof, C.W., Buckley, J., et al., 1995, ApJ 445, 227
Blandford, R.D., Königl, A., 1979, ApJ 232, 34
Bridle, A.H., Perley, R.A., 1984, Ann. Rev. A&A 22, 319
Camenzind, M., 1990, Rev.Mod.Astron. 3, 234
Courant, R., Friedrichs, K.O., 1948, *Supersonic Flow and Shock Waves*, Interscience Publishers, New York
De Jager, O.C., Stecker, F.W., Salamon, M.H., 1994, Nature 369, 294
De Zotti, G., Francheschini, A., Mazzei, P., Granato, L., Danese, L., 1995, Invited Review at Gifco, Oct 26-28, 1994, Rimini, Italy, in press
Drury, L.O'C., 1983, Rep.Prog.Phys. 46, 973
Dwek, E., Slavin, J., 1994, ApJ 436, 696
Ellison, D.C., Baring, M.G., Jones, F.C., 1995, ApJ 453, 873
Falomo, R. Ghisellini, G., Maraschi, L., et al., 1995, Adv.Sp.Res. 15, 69
Fichtel, C.E., Bertsch, D.L., Chiang, L., et al., 1994, ApJS 94, 551
Gould, R.J., Schrèder, G., 1966, Phys.Rev.Lett. 16, 252
Harris, D.E., Carilli, C.L., Perley, R.A., 1994, Nature 367, 713
Hartman, R.C., 1995, private communication
Karle, A., et al. 1995, Astropart. Phys. 4, 1
Kerrick, A.D., Akerlof, C.W., Biller, S.D., et al., 1995a, ApJ 452, 588
Kerrick, A.D., Akerlof, C.W., Biller, S.D., et al., 1995b, ApJ 438, L59
Kirk, J.G., Heavens, A.F., 1989, MNRAS 239, 995
Kirk, J.G., Schneider, P., 1989, A&A 225, 559
Kirk, J.G., 1992, in: *Particle acceleration in cosmic plasmas*, Proc. of a Workshop at Bartol Research Inst., Newark, DE, Dec. 4-6, 1991, p. 294
Krülls, W., 1990, Dissertation, Rheinische Friedrich-Wilhelm Universität Bonn, Germany
Kühn, M., Dissertation, 1994, Christian-Albrechts-Universität Kiel, Germany
Lichti, G.G., Balonek, T., Courvoisier, T.J.-L., et al., 1995, A&A 298, 711
MacMinn, D., Primack, J., 1996, Space Sci. Rev. 75, 413
Macomb, D.J., Akerlof, C.W., Aller, H.D., 1995, ApJ 449, L99
Madau, P., Phinney, E.S., 1996, ApJ 456, 124
Malkov, M.A., Völk, H.J., 1995, A&A 300, 605
Mannheim, K., Krülls, W., Biermann, P.L., 1991, A&A 251, 723
Mannheim, K., 1993a, A&A 269, 67
Mannheim, K., 1993b, Phys. ReV. D 48, 2408
Mannheim, K., 1995, Astroparticle Physics 3, 295
Mannheim, K., 1996, Space Sci. Rev. 75, 331
Maraschi, L., Grandi, P., Urry, C.M., et al., 1994, ApJ 435, L91

Montigny, C. von, Bertsch, D.L., Chiang, J., et al., 1995, ApJ 440, 525

Petry, D., et al., 1995, in: Proc. of the 4th Workshop "Towards a major atmospheric Cherenkov detector IV", Padua, C. Cresti (ed.), p. 230

Plaga, R., 1995, Nature 374, 430

Protheroe, R. J., Stanev, T., 1993, MNRAS 264, 191

Punch, M., Akerlof, C.W., Cawley, M.F., et al., 1992, Nature 358, 477

Quinn, J., Akerlof, C.W., Biller, S., et al., 1996, ApJ 456, L83

Salamon, M.H., Stecker, F.W., De Jager, O.C., 1994, ApJ 423, L1

Schneider, P., Kirk, J.G., 1989, A&A 217, 344

Sikora, M., Kirk, J.G., Begelman, M.C., Schneider, P., 1987, ApJ 320, L81

Stecker, F.W., De Jager, O.C., Salamon, M.H., 1992, ApJ 390, L49

Thompson, D.J., Bertsch, D.L., Dingus, B.L., et al., 1995, ApJS 101, 259

Urry, C.M., Padovani, P., 1995, PASP 107, 803

Valtaoja, E., Teräsranta, H., 1995, A&A 297, L13

van Putten, M.H.P.M., 1995, Nature, submitted

Webb, G.M., 1989, ApJ 340, 1112

Westerhoff S., et al. 1995a, Astropart. Phys. 4, 191

Westerhoff, S.,et al. (HEGRA collab.), 1995b, in: Proc. 24th Int. Cosmic Ray Conf., Rome, Vol.3, p. 230

Zdziarski, A.A., Krolik, J.H., 1994, ApJ 409, L33